Robotics and Computer Integrated Manufacturing 66 (2020) 101995

Contents lists available at ScienceDirect

Robotics and Computer Integrated Manufacturing

journal homepage: www.elsevier.com/locate/rcim

A voice activated bi-articular exosuit for upper limb assistance during lifting tasks

Yongtae G. Kim[a], Kieran Little[a], Bernardo Noronha[a], Michele Xiloyannis[b], Lorenzo Masia[1,c], Dino Accoto[*,1,a]

[a] Robotics Research Centre, Nanyang Technological University, 50 Nanyang Avenue, Singapore
[b] Sensory Motor-Systems (SMS) Lab at ETH Zürich, Tannenstrasse 1, Zürich, Switzerland
[c] Institut für Technische Informatik (ZITI) Heidelberg University, Im Neuenheimer Feld 368, 69120 Heidelberg, Germany

ARTICLE INFO

Keywords:
Exosuit
Wearable Robot
Voice Recognition
Underactuated Mechanism
Industrial robotics

ABSTRACT

Humans are favoured to conventional robotics for some tasks in industry due to their increased dexterity and fine motor skills, however, performance of these tasks can result in injury to the user at a cost to both the user and the employer. In this paper we describe a lightweight, upper-limb exosuit intended to assist the user during lifting tasks (up to 10kg) and while operating power tools, which are common activities for industrial workers. The exosuit assists elbow and shoulder flexion for both arms and allows for passive movements in the transverse plane. To achieve the design criteria an underactuated mechanism has been developed, where a single motor is used to assist two degrees of freedom per arm. In the intended application, the hands are generally busy and cannot be used to provide inputs to the robot, therefore, a voice-activated control has been developed that allows the user to give voice commands to operate the exosuit. Experiments were performed on 5 healthy subjects to assess the change in Muscular Activation (MA), inferred through Electromyography (EMG) signals, during three tasks: i) lifting and releasing a load; ii) holding a position and iii) manipulating a tool. The results showed that the exosuit is capable of reducing EMG activity (between 24.6% and 64.6%) and the recognition rate (94.8%) of the voice recognition module was evaluated.

1. Introduction

Industrial environments are associated with high rates of accidents and Work-Related Musculoskeletal Disorders (WMSD) as there are many tasks that benefit from human operation, despite the ongoing trend of robotic automation uptake in industry. Humans can provide a combination of mobility, decision making and fine motor skills, which makes them invaluable for handling tasks such as holding and manipulating heavy loads, and repetitive hand or arm movements [1]. Current research efforts are focusing on developing collaborative robots and wearable assistive devices which both have the potential to assist the worker and directly reduce the risk of WMSD, increase productivity and reduce the health compensation required by the employer [2].

Collaborative robots are designed to work in conjunction with humans by allowing the device to withstand the payload of heavy and cumbersome items [3]. Typical mechanisms for collaborative robots include: linkage mechanism stemming from the ceiling, which can move in a planar workspace [4]; cable-suspended robots [5]; or collaborative robotic arms [6]. The disadvantage of these systems is the lack of portability due to their fixed workspace and the lack of intuitive human control. In comparison, wearable devices have the advantage of being extremely portable and have the potential to implement a very intuitive human-machine interface. Exoskeletons are an example of wearable robots that can provide support to the muscular-skeletal system of the user and can be categorised as either active or passive. Active devices benefit from actuators to add power to the wearer, while passive devices utilise elastic components to cyclically store and release energy, e.g. to provide gravity compensation for the weight of the limb. Active, rigid exoskeletons are often heavy and cumbersome, which can result in poor ergonomics and safety limitations. Conversely, passive devices are often more lightweight; however, they can have reduced functionality due to the lack of actuation [7]. Current applications of

Abbreviations: MVC -, Maximum Voluntary Contraction; BB -, Biceps Brachii; AD -, Anterior Deltoid; MA -, Muscular Activation; VRM -, Voice Recognition Module; HMI -, Human Machine Interface; DoF -, Degree of Freedom; WMSD -, Work-Related Muskuloskeletal Disorders; EMG -, Electromyography

* Corresponding author.
E-mail address: daccoto@ntu.edu.sg (D. Accoto).
[1] Equal contribution

https://doi.org/10.1016/j.rcim.2020.101995
Received 19 November 2019; Received in revised form 17 March 2020; Accepted 23 April 2020
Available online 15 May 2020

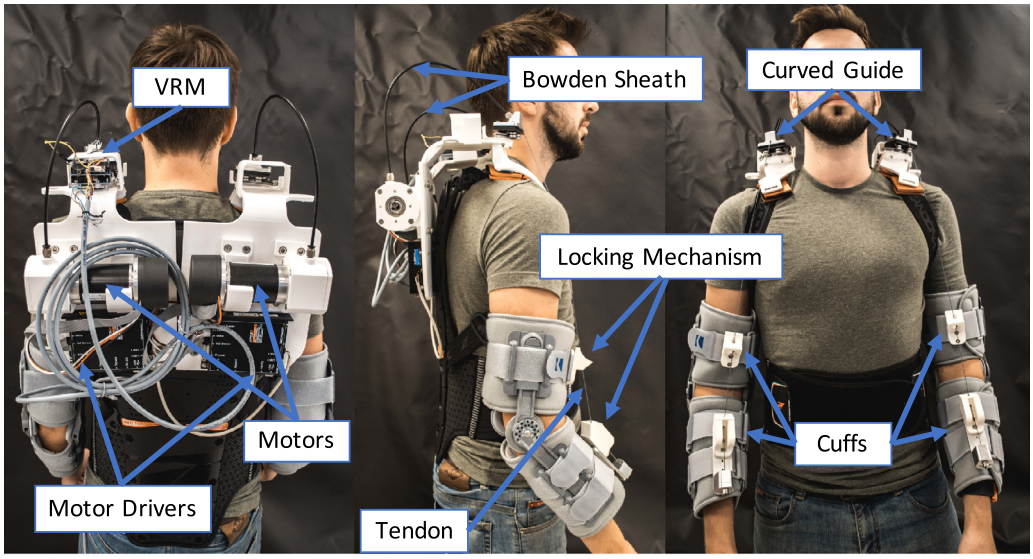

Fig. 1. Overview of the exosuit. The exosuit supports 4 Degrees of Freedom (DoF) with underactuated mechanisms and a Voice Recognition Module (VRM).

exoskeletons include assistance during industrial tasks and rehabilitation from neuro-muscular disorders [8].

Currently, passive exoskeletons dominate the market whereas active ones are mostly at development stages [7]. The Personal Lift Augmentation Device (PLAD) [9] is a pioneering passive exoskeleton used in industry. The device is composed of elastic elements that store energy when bending the trunk and release this energy upon lifting. Huysamen et al. [10] have recently developed a passive upper limb exoskeleton to assist the performance of static overhead tasks. Muscular Activity (MA) was significantly lower with the device while holding a load (49 % for the biceps brachii and 62% for the medial deltoid). Theurel et al. [11] assessed the physiological consequences of using EXHAUSS Stronger ®, a comercial upper limb passive exoskeleton, while performing lifting, carrying and stacking/unstacking of a load. They observed a significant reduction in the anterior deltoid muscle activity (− 54%) during lifting and stacking tasks.

Several active exoskeletons that are designed to support the upper limbs exist, although only the Muscle Suit has been shown to significantly decrease MA [12]. The Muscle Suit provides assistance in shoulder, elbow and trunk flexion in the sagittal plane using McKibben artificial muscles. The device was shown to reduce the anterior deltoid activity by 20 ∼ 35% in dynamic lifting and static holding. There have also been efforts to develop a device that can act as both passive and active: Otten et al. [13] developed an exoskeletal system that can operate at different assistance levels by triggering a button on the grip of the tool being operated. Looze et al. [1] have highlighted user discomfort and device weight/size as some of the disadvantages of active exoskeletal devices. These devices are heavy, which often leads to user discomfort, as actuators are often the heaviest component and typically one actuator is necessary for each degree of freedom. As an example, even though the Muscle Suit uses lightweight actuators, it weighs 9 kg.

Soft exoskeletons, or exosuits, apply assistive torques to human limbs through compliant material and are more lightweight compared to exoskeletons with similar functionalities. In addition, the inherent compliance of exosuits allows greater adaptability to the human body, which results in improved ergonomics. Exosuits use actuation strategies that allow the user to benefit from assistance without restricting their versatility in motion control. Xiloyannis et al. [14,15] developed an exosuit using a wire mechanism that aids elbow flexion by compensating for the gravitational torque that resulted in a significant reduction in MA (65%) and biological torque (59%). Zhang et al. [16] have published preliminary results on an exosuit that is actuated by cables meant for carrying heavy loads. They developed a mechanism for maintaining the tension in the cables when the user changes position, and optimised the position of the anchor points according with the force exerted on the body.

An intuitive human-machine interface (HMI) to ease the operation of industrial wearable devices is of paramount importance for real-world applications [17]. The interface should allow the user to impart motor commands in a natural and unobtrusive way, possibly without requiring actions (e.g. pushing buttons) that could interfere with the execution of the specific task. Myoelectric activity control and voice command are options for hands-free control as they are both independent from human movement. However, myoelectric control requires additional sensors to be worn by the user that increases the complexity of the system. In addition such method is not reliable due to the variability between and within subjects [18]. Voice command control is a simple and intuitive implementation of an intention detection control system. This control is not new in the field of industrial robots control [19], but it can benefit from the recent advancements in voice recognition technology. Overall, HMIs based on natural speech have a great potential in the field of wearable robotics for industrial applications, because they leave the hands free for the execution of the task and do not involve high cognitive loads.

In this paper, we present a lightweight, underactuated, active, upper-limb exosuit which is the second version of our initial prototype [20] and it is intended for providing assistance to industrial workers (Figure 1). The HMI is based on an intuitive Voice Recognition Module (VRM) providing inputs to a low-level position control system. We evaluated the VRM-based control system in terms of recognition and success rate. The change in MA of the biceps brachii and anterior deltoid, with and without assistance from the exosuit, is analysed during lifting, holding and manipulation tasks.

2. Materials and Methods

2.1. Mechanical Design

2.1.1. Design criteria

The device was designed with the aim to assist the arm elevation of the wearer, which involves flexing of the shoulder and elbow, without restricting the natural mobility and fine motor skills of the user. To achieve this aim the device must adhere to these criteria:

- Ability to lift a 10kg load
- Lightweight (Device weight ≤ Maximum load)

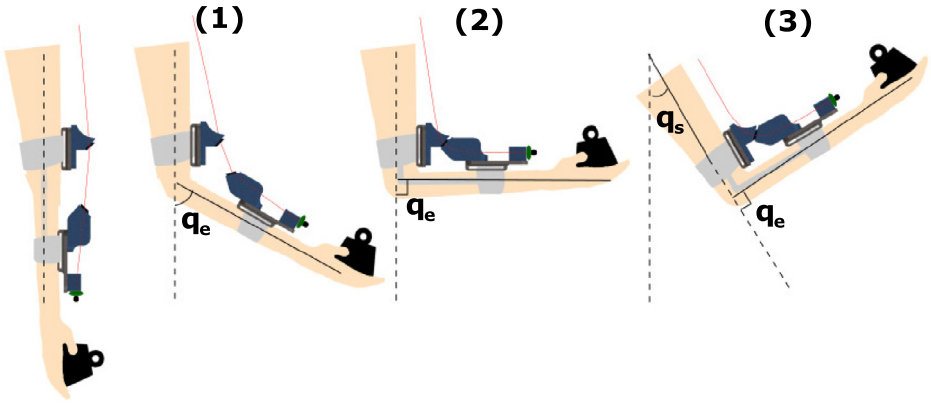

Fig. 2. The underactuated mechanical architecture of the exosuit. The elbow (q_e) is flexed by pulling a wire until it reaches 90°. When q_e = 90° the elbow angle is locked and the assistance is transferred to the shoulder joint (q_s) using the same wire. The lower part (attached to the forearm) is lifted until it reaches the locking position and then the upper part (attached to the upper arm) is lifted after locking. Before locking-(1), the lower part approaches the locking configuration due to wire tension. After locking-(2), the shoulder joint starts flexing due to wire tension. (3) shows the shoulder joint flexion after locking. A load cell (green) is installed at the end of the wire for measuring the wire tension.

- Adaptable to different lifting postures and situations
- Support the shoulder and elbow joints

The target maximum load was selected to be 10kg, as this is the recommended load limit for light lifting tasks that are classified as "difficult" [21].

2.1.2. Exosuit overview

The exosuit [20] is presented in Figure 1 and the configuration of the device during lifting is shown in Figure 2. The device uses a wire-driven mechanism to apply a torque to the elbow and shoulder joints using Bowden cables (Shimano inc) that allowed the actuation unit to be moved away from the joints, while limiting friction in the transmission. The torque of the actuator is transmitted via the tension of the wire, which is winded by rotation of the motor. The estimated required torque for the device was calculated using a planar 2 DoF manipulator model with a point mass load (Figure 3) using anthropometric data from [22] (Table 1). This allowed the maximum required torque and wire tension to be calculated, and the motors (EC60 Flat Brushless 100W, Gear Ratio 126:1, Maximum Continuous Torque 21Nm, driver EPOS2 50/5, Maxon) and the wire (HERCULES - 250 LB, 1.0mm, 8PLYS) to be selected accordingly. The length of the wire could also be estimated by the revolutions of the motor needed for actuation across all the ROM of the device, measured by a incremental rotary encoder (ENC MILE 512IMP, resolution: 2048 ppr). Assuming the end-point of the Bowden-cable is fixed, the rotation of the motor was measured by motor counts θ_m.

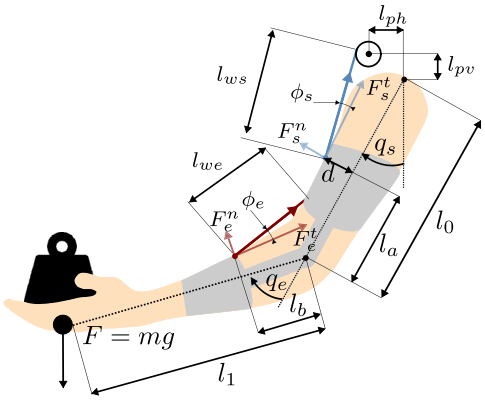

Fig. 3. Planar model of the human arm in the sagittal plane and geometry of wire routing. q_s: shoulder flexion angle (measured from the vertical axis of the user); q_e: elbow flexion angle (measured from the axis of the upper arm); l_0: length of the upper arm; l_1: length of the forearm + gripping length; l_a, l_b: anchor points distances from the elbow joint; l_{ph}, l_{pv}: wire origin position at the shoulder joint; m: mass of the load; g: gravitational constant; d: vertical distance between anchor point and the center of upper arm; l_{ws}: wire length between shoulder anchor point and the wire origin position.

Table 1
List of measurements used in the model used for calculating the specifications of the exosuit.

Variable	Length (mm)
l_0	370
l_1	470
l_a, l_b	100
l_{ph}, l_{pv}	100
d	80

The exosuit (Figure 4) consists of three modules: back module, left arm module; right arm modules. The back module is made of PLA and

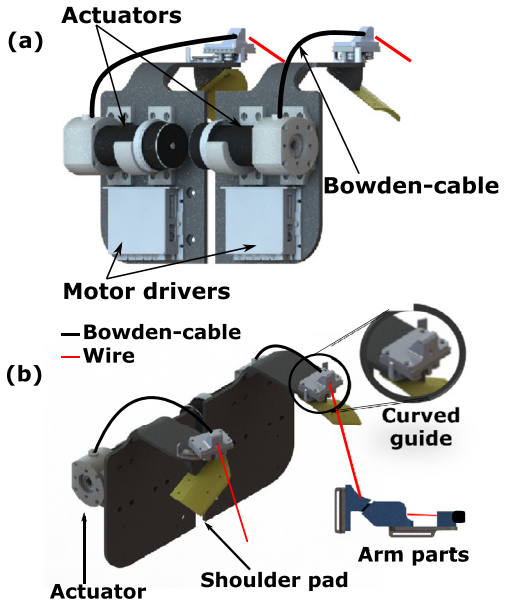

Fig. 4. Schematic of the exosuit. (a) The back view of the exosuit. (b) The front-upper view of the exosuit.

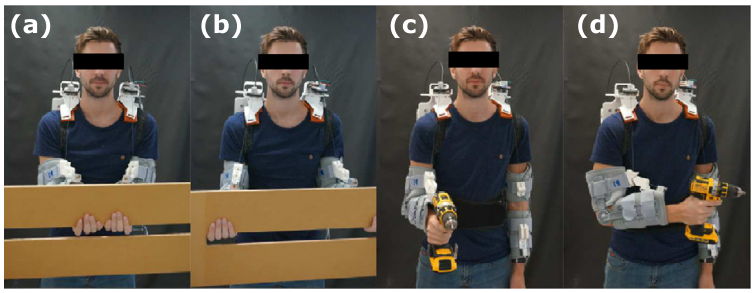

Fig. 5. Examples of the permitted postures of the exosuit. The wearer can use a variation of postures for lifting and holding. (a) and (b) show two examples of lifting a woodblock: both hands in a narrow grip (a) or a wide grip (b) are possible with the passive DoF on the shoulder. (c) and (d) show two examples of handling an industrial tool that the wearer can point forwards (c) or sideways (d) with continuous exosuit support.

houses the actuators, motor drivers and Voice Recognition Module (VRM) while the arm modules are adapted from an upper limb orthosis (AM-KG-AR/1R, REH4MAT). The Bowden sheath is anchored to a rotating anchor point located above the shoulder that behaves as a passive joint, allowing for passive internal/external rotation of the shoulder joint (Figure 4.(b)). This passive rotation is achieved by the sliding anchor point, which is placed on a curved guide. The position of this passive joint should intersect with the axis of the upper arm while the center of curvature of the guide rail should be centered about the axis of the upper arm. This mechanism allows for freedom of hand movement for the wearer that allows different lifting postures (Figure 5) and therefore improves the ergonomics of the device. From the anchor point, the wire is passed though the locking mechanism and routed at the forearm module, which allows for flexion of the elbow and shoulder joints. A detailed description of this mechanism can be found below.

2.1.3. Locking mechanism

The mechanism utilizes a mechanical locking whereby the wire is guided through a rigid guide placed on the upper arm cuff and one on the forearm cuff, and then attached to an anchor point (Figure 2). When the wire is wound, the elbow is flexed until both the rigid guides come into contact, this configuration shall herein be referred to as "locked configuration", at which time the shoulder starts flexing. The tendon applies a torque to the shoulder and elbow joints and the resultant motion is split due to their resistances: after the forearm reaches the locked configuration, the mechanism behaves as a single rigid body due to the high stiffness of the elbow joint, and the tension of the wire generates a torque at the shoulder joint. The locked angle can be adapted to allow a variety of different postures appropriate for different tasks, such as handling tools, holding a position or lifting loads. In the current design, the locking angle was chosen to be $\bar{q_e} = 90°$. This mechanism allowed the use of two, rather than four motors, to actuate four DoF. As motors are often the heaviest component of a wearable robot, this allowed the lightweight criteria to be achieved and improved the power-to-weight ratio of the device. Moreover, decreasing the weight of the device results in improved ergonomics. The total weight of the device is 7.5kg.

2.2. Voice Recognition System

The VRM (EasyVR 2 Shield, Veear-ROBOTECH SRL) was integrated with an Arduino Uno board to detect the user's voice commands. This VRM has a set of available words and allows for the creation of user-defined commands. Although there is an option to create custom commands, this would mean that a comprehensive training of the voice recognition algorithm would be necessary, involving different speech accents and conditions. Instead, it was decided that the pre-trained commands would be used, as the provided wordset had already been extensively trained and was sufficient for the intended application.

The chosen voice wordset consists of the following commands: [UP, DOWN, LEFT, RIGHT, FORWARD, BACKWARD] (Table 2). The chosen voice commands FORWARD and BACKWARD are used to flex and release both arms and [UP, DOWN] commands are used to adjust the elevation of each arm. The FORWARD and BACKWARD commands switch the lengths of the wires between two fixed configurations that can be adjusted by the user. Due to the inevitable delay between speech and recognition, we decided to pre-define the target points: Configuration 1 (C1) is defined, by default, as having the arms fully extended and Configuration 2 (C2) can be customised to a user-defined configuration (described in terms of the wire winding value e.g. $\theta_m(C2) = 10^6$ counts, corresponding approximately to $q_e = 90°$, $q_s = 30°$). The [UP,-DOWN] commands are used to wind/release the wires by a small amount set as 2.4 cm, which corresponds to $\Delta\theta_m = 10^5$ counts. The commands LEFT and RIGHT are used to activate/deactivate the left and right arms (one-handed operation), respectively. If the arms are in C1, the [LEFT,RIGHT] commands will bring the respective arm to C2. If the arms are already in C2, these commands will select the respective arm so that the [UP,DOWN] commands can be used for adjusting the elevation.

Table 2
List of commands for the exosuit control. [FORWARD, BACKWARD] are used to actuate both arms together, [LEFT, RIGHT] are used to switch between arm selection and to actuate an individual arm, and [UP, DOWN] are used for fine tuning the elevation.

Command	Action
FORWARD	Lift arm
BACKWARD	Release arm
UP	Add offset to selected arm
DOWN	Subtract offset to selected arm
LEFT	Select/deselect left arm
RIGHT	Select/deselect right arm

The actuation of the device predominantly alternates between predefined positions and the simplest way to implement this is using position control. One could use force/torque control instead, however sensors to measure the upper arm angles would need to be implemented. For simplification of the device, it was decided that such sensors would not be used, and an open-loop position control paradigm was adopted. Furthermore, although torque control presents a higher precision and speed over position control, it requires that the dynamic parameters of the robots be modeled accurately [23]. Due to the compliant nature of the device, this is very difficult to perform. A scheme illustrating the control paradigm of the device can be found in Figure 6.

2.3. Experimental Design

2.3.1. Voice Recognition Interface

The voice recognition experiment was performed by a group of 5 subjects (Age: 27.6 $\pm$ 3.21 years, all males). The participants were presented each voice command [UP, DOWN, LEFT, RIGHT, FORWARD, BACKWARD] on a screen and asked to repeat the command. Each subject received the same order and number (120 trials) of each command to achieve comparable results. The test was performed in a quiet environment ($<$ 45dB).

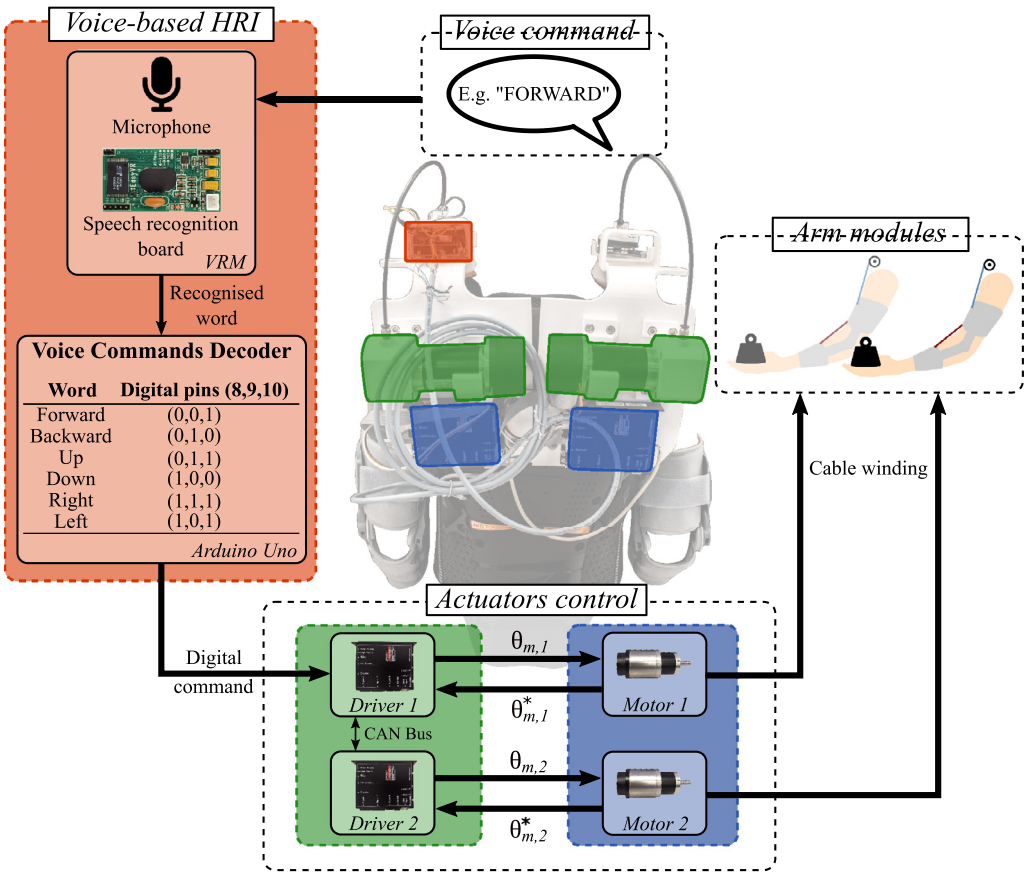

Fig. 6. Architecture of the voice-activated control. The input to the VRM is the voice command spoken by the user. The command is interpreted by a VRM (Easy VR2 shield by VeeaR). The recognised word is passed to the Arduino Uno, where the voice command is decoded. This command is output from the Arduino Uno through 3 of its digital pins in the form of a binary triplet, and input to motor driver 1 (EPOS2 by Maxon Motor). Motor driver 1 acts as a master and driver 2, identical to driver 1, as a slave. The two drivers are connected via CAN bus. The binary triplets are decoded into reference positions in driver 1. The reference position for motor 2 is communicated to driver 2. Each driver implements a PID position control at 1kHz for the respective motor. $\theta_{m,i}$: reference position (motor counts) sent to the motor i ($i = 1, 2$); $\theta^*_{m,i}$: actual position (motor counts) read by the encoders. The colour scheme adopted in the figure shows where each module is located in the exosuit.

2.3.2. Manual Tasks

To evaluate the performance of the exosuit, a set of experiments were designed based on tasks that are ubiquitous in an industrial environment:

1. Lifting and releasing a load [11];
2. Holding a load at a fixed position [10];
3. Manipulating an industrial tool [13].

The manual experiments were performed by a new group of 5 healthy subjects (Age: 25.2 ± 1.10 years, height: 179.8 ± 4.09 cm, weight: 74.6 ± 8.26 kg, all males). The procedures were in agreement with the Declaration of Helsinki and approved by the Institutional Review Board at Nanyang Technological University. The experiments aimed to evaluate the device through measurement of the changes in muscular activation (MA) between powered and unpowered conditions and were measured using electromyography (EMG). The EMG sensors (200Hz, Trigno EMG, Delsys) were attached according to the SENIAM recommendations [24] to the Biceps Brachii (BB) and Anterior Deltoid (AD) muscles, which are the most prominent for elbow and shoulder flexion. The Maximum Voluntary Contraction (MVC) of the target muscles was manually collected at the beginning of each manual experiment to standardize the results across subjects. For measuring the MVC, the subjects were asked to flex the arm and forearm (for the AD and BB's MVC, respectively) with the maximum force possible against a fixed object. It was measured three times for each target muscle with a short break between measurements to avoid fatigue.

The kinematics of the device was evaluated from q_e and q_s; q_e was measured using an encoder (E6A2-CWZ32, OMRON, 500 ppr) that was attached between the upper-arm and forearm modules, used only for evaluation of the device. The shoulder flexion angle (q_s) was estimated according to the planar model (Figure 3) by measuring θ_m and finding the motor encoder position at the lock point (Section: 2.3.2). The tension of the wire was measured using a load cell (LTH300, FUTEK), which was attached at the end of the wire. The voice recognition interface was not active during the manual tasks as it was important that the total time of each repetition was the same between subjects.

Calibration and Familiarization

First, the participant donned the exosuit and the motor angle at the locking configuration $\theta_m(\bar{q_e})$ was recorded. The wire length during shoulder flexion (Δl_{ws}) was calculated from the motor displacement ($\Delta\theta_m$) using the radius of the pulley at the actuator (r_{pulley} = 10mm). The shoulder flexion angle (q_s) was calculated using Δl_{ws} and the arm model (See Appendix Appendix A).

The configurations C1 and C2 were set according to the $\theta_m(\bar{q_e})$ to allow an approximation of the joint angles:

- C2: The shoulder is flexed 30° from the locking configuration by rotating the motor − 241200 counts from $\theta_m(\bar{q_e})$.
- C1: The motor rotated $\Delta\theta_m = 10^6$ counts from C2 such that the arms extend.

Following the calibration, the exosuit was actuated between C1 and C2 for three repetitions to familiarize the user with the device.

Lift and Release The exosuit was set to follow predefined targets (θ_{mi}, θ_{mf}) with motor velocity ($\dot{\theta_m}$) of 2500 rpm (19.84 rpm, after reduction, wire winding speed ($\dot{l_w}$) = 2.1cm/sec) that included a lift phase and a release phase. In the lift phase the exosuit followed a trajectory that started at C1 and finished at C2. The elbow flexion was set to prevent contact between the arm of the wearer and trunk. Configuration 2 was maintained for 3s before the release phase and the trajectory of the release phase was the inverse of the lifting phase. In unpowered lifting/releasing, a reference motion was displayed on a screen to synchronize the trajectory between conditions. The subjects conducted powered

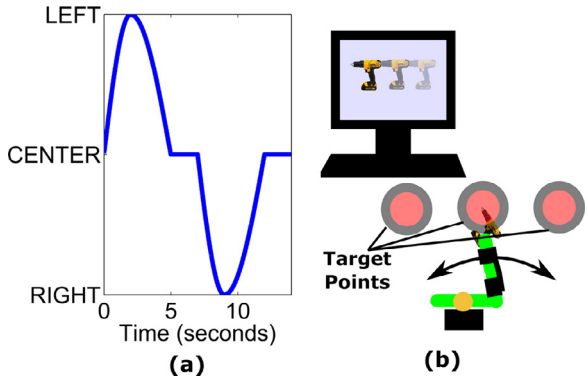

Fig. 7. Experimental setup with video reference. (a) Subjects moved their arm to the left in 2 s, then returned in 3 s, then waited for 2 seconds, then moved their arm to the right in 2 s, then returned in 3 s, and then waited for 2 s. (b) A video guided the user to move the power tool.

lifting/releasing prior to unpowered lifting/releasing to learn the trajectory intended in the task.

Hold Position The participants were given a 7kg woodblock to hold for 15s at C2. To match the exosuit position in the unpowered experiment to the powered experiment, the participants were asked to remain at C2 after the wire tension was released.

Manipulation The participants were asked to manipulate a power tool (Hand drill, DCD790D2, 3.8kg) to reach three target points. These points were shown in a video that illustrated the tool moving between three fixed points aligned horizontally (Figure 7.(a)). The target positions were placed in the transverse plane (25cm apart) at approximately the shoulder height of the user. Participants were instructed to manipulate the power tool only by internal/external rotation of the upper arm, to assure sole reliance on the passive DoF of the device. This experiment included three repetitions and was repeated in both powered and unpowered conditions (Figure 7.(b)).

2.4. Data Analysis

The EMG signals were pre-processed using a second-order low-pass Butterworth filter with 10Hz cut-off frequency. The Root Mean Square (RMS) of the amplitude was computed before calculating the percentage change of mean MA between powered and unpowered conditions.

The recognition rate of the VRM was defined as the ratio between the number of successfully recognized trials and the total number of trials. The success rate for each attempt i was defined as the percentage of trials that needed i or less attempts to be completed successfully.

Normality of the EMG data was checked using a one-sample Kolmogorov-Smirnov test, and it was verified that all data followed a normal distribution. A one-sided paired t-test was performed on the mean MA differences between powered and unpowered conditions with a significance level of $\alpha = 0.05$. Values are presented as mean $\pm$ standard deviation.

3. Results

3.1. Voice Recognition Test

The results of the voice recognition experiment are shown in Figure 8. Six hundred trials were performed, and the average recognition rate of the VRM was 94.8 $\pm$ 5.3%, with the highest one being 100% for the LEFT command and the lowest one being 84% for the RIGHT command.

The success rate increased with the number of attempts, starting from 94.8% for the first attempt, 98.7% for the second and 99.7% for the third attempt (Table 3). This means that 94.8% of trials needed only 1 attempt, 98.7% needed 2 or less attempts and 99.7% needed 3 or less attempts.

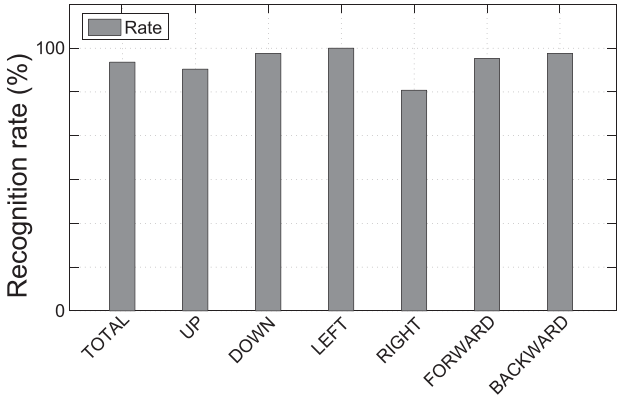

Fig. 8. The results of the voice recognition test. Six hundred (600) trials of voice recognition (100 trials per each command) were completed. The recognition rate of [LEFT] was the highest (100%) of all commands and the recognition rate [RIGHT] was the lowest (84%) of all commands.

Table 3
Voice recognition success rates according to number of attempts needed until a successful trial.

Attempts	1	2	3
Success rate	94.8	98.7	99.7

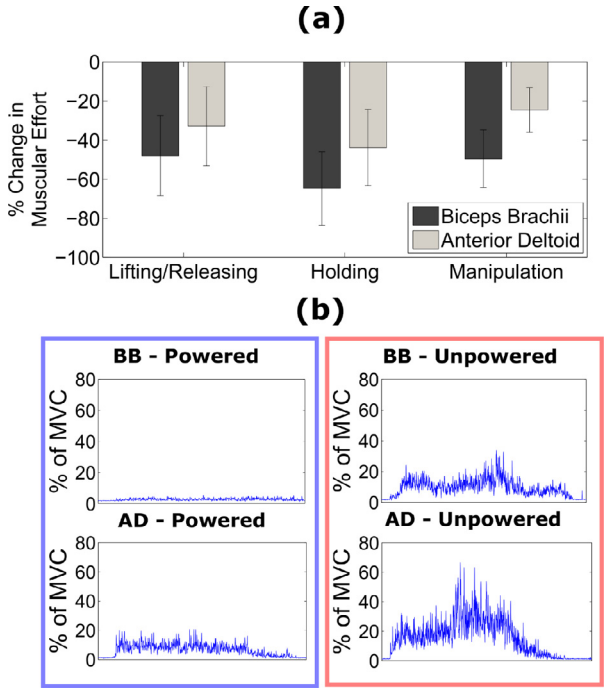

Fig. 9. Experimental results of the manual experiments. (a) Mean percentage change of MA for each task across all subjects. The values are presented together with the standard deviation. (b) Example of EMG signal (as a percentage of the MVC) during the performance of the lift and release experiment by one subject, for the powered/unpowered conditions and for each muscle. Top left and bottom left correspond to powered condition for the BB and AD, respectively, and top right and bottom right correspond to unpowered condition for the BB and AD, respectively.

3.2. Manual Experiments

Figure 9 presents the results of the manual experiments and

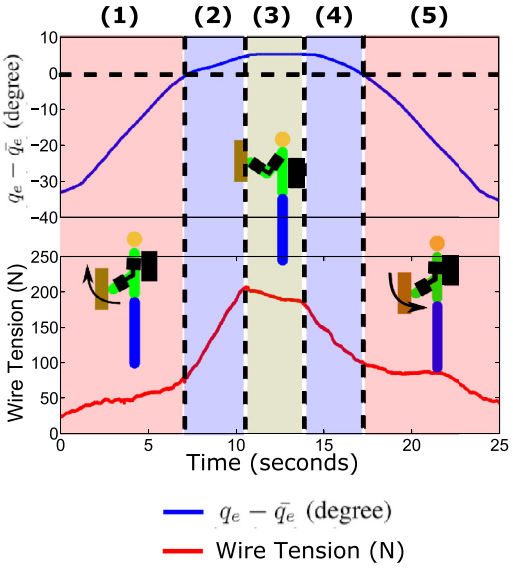

Fig. 10. The mean of the joint angle ($q_e - \bar{q}_e$) and wire tension during the lifting and releasing experiment for one subject. The wire tension (red) increases when the wire supports both the shoulder and elbow joints. (1) Elbow flexion; (2) Shoulder flexion; (3) Holding; (4) Shoulder extension; (5) Elbow extension.

Figure 10 shows an example of the joint angles and wire tension during the lifting and releasing experiment. In the lifting and releasing experiment, both the BB and the AD were significantly less activated ($-$ 48.0 $\pm$ 20.5%, $p = 0.0007$ and $-$ 32.9 $\pm$ 20.3%, $p = 0.0459$, respectively) in the powered condition. In the holding experiment, the BB and the AD showed significantly reduced activation ($-$ 64.7 $\pm$ 18.8%, $p < 0.0001$ and $-$ 43.8 $\pm$ 19.5%, $p = 0.0093$, respectively) in the powered condition in comparison with the unpowered condition. In the manipulation experiment, the MA of the AD was significantly lower in the powered condition ($-$ 24.6 $\pm$ 11.3%, $p = 0.0135$). The BB also had a lower activation in the powered condition, although this change was not statistically significant ($-$ 49.6 $\pm$ 14.7%, $p = 0.0754$).

4. Discussion

The exosuit was evaluated by measuring the recognition and success rate of the VRM and the change in muscular effort of the user in powered and unpowered conditions for three experiments: lifting/releasing a load, holding a load, and manipulating a power tool.

4.1. Performance evaluation

The VRM performed well, with recognition rates being on average close to 95%. These results are comparable to the ones obtained in other studies, such as rates equal to or higher than 90% by Barkana et al. [25] and around 99% by Poncella et al. [26], which shows the VRM used in our device has high recognition accuracy. Furthermore, the success rate was also very high, being around 95% for the first attempt, and increasing to approximately 100% in the third attempt. This increase was already expected since it is normal to fail less times at a certain task as the number of attempts increases.

The performance of the exosuit during manual experiments can be compared with existing wearable devices; Theurel et al. [11] evaluated the performance of a wearable system by measuring the MA of the AD in a lifting/releasing task and found a significant change of $-$ 54% when using the device, while we obtained a change of AD of $-$ 32.9%. Huysamen et al. [10] evaluated the performance of a passive wearable device during a holding experiment by measuring the MA of the BB and reported a significant change of $-$ 49%, while we measured a $-$ 64.7% change for the BB and $-$ 43.8% for the AD. Otten et al. [13] reported that their wearable system significantly changed the MA of the AD muscle between $-$ 39.1% and $-$ 58.2% during a manipulation task, while we have shown a $-$ 24.6% change of AD. We found a greater change in MA for the BB than for the AD; this is likely due to the compensatory torque generated at the shoulder when holding a load to resist shoulder extension [27]. This torque is created by the user both in the powered and unpowered conditions, since the exosuit does not aid shoulder flexion before the elbow is locked. The result of this is that the MA of the AD is less reduced than the BB throughout the total lifting motion.

4.2. Design evaluation

The design employs a locking mechanism that allows a change in device dynamics to actuate the elbow and then the shoulder joint. The change in torque occurs at the lock configuration, which can be identified from the lift and release experiment as when the gradient of the wire tension increases (Figure 10). It can be observed that the elbow joint starts to 'overflex' after the locked configuration ((2) in Figure 10), approximately 6°. This effect can be explained by the inherent compliance of the device, which allows for the locking mechanism to become nonparallel with the axis of the upper arm and forearm. This occurs similarly during the release phase, although it is more difficult to detect the locked configuration due to the gradual change in gradient ((4) transitions into (5) in Figure 10). This effect suggests that there were inaccuracies in the calculation of q_s from the model however, these inaccuracies are only relevant to the kinematics of the device and not for the control of the device.

The mechanism is bi-articular, spanning the elbow and shoulder joints, similarly to the BB. The BB aids flexion of the elbow and also contracts during shoulder flexion although the exact role of the muscle for shoulder function is still unclear. Current studies show that the BB applies an insignificant torque compared to the anterior deltoid for shoulder flexion, it is instead theorised that the BB affects the dynamic stability of the joint [28]. The bi-articular mechanism presented here, unlike the BB, supports shoulder flexion due to the change in joint resistance when the elbow becomes locked (Figure 2). There have also been other exosuits designed using the same bi-articular principle for lower limb assistance [29].

This device is designed to be used by multiple users, therefore the arm modules allow for donning by users with different forearm and upper arm sizes. However, the robustness of the model used for estimating the joints angles from the motor counts must be evaluated to ensure that there were no significant differences in the configurations adopted by the subjects during the experiments. For this, a sensitivity analysis was performed on the arm model to investigate inaccuracies that are introduced in the calculation of joint angles due to variation in the anthropometric parameters of each participant. The only anthropometric measurement that influences q_e and q_s is the upper arm length, which for this analysis was considered to vary between the 5th and the 95th percentile of the Singaporean male population [22]. The variation in elbow angle, Δq_e, due to variation in upper arm length Δl_0 is calculated using eqs. (A.6) and (A.7), whereas the variation in shoulder angle, Δq_s, due to Δl_0 was calculated by numerical approximation of the inverse function of eq. (A.1). The results of the analysis showed that for $\Delta l_0 \in [0, 0.10]$ m, elbow and shoulder angle vary in the intervals $q_e \in [0, 1.97]^\circ$ and $q_s \in [0, 0.35]^\circ$. The change in angle that results from variation in the upper arm length ($0.35^\circ \sim 1.97^\circ$) is considerably smaller than the change in angle that results from the compliance of the device (6°). Therefore, it can be assumed that the inaccuracy in q_e and q_s is insignificant and the design of the device is robust regarding the variability in each users' anthropometry.

4.3. Future improvements and limitations

There are some limitations to the device that should be considered

in future iterations of the design. First, the locking mechanism has a number of advantages such as reducing the number of actuators, however, this means that the elbow and shoulder flexion cannot be actuated individually. In addition, it was assumed that, while the elbow has not reached the locked configuration, the shoulder motion during elbow flexion is negligible due to intrinsic dynamic properties of the arm [27], however, if the weight of load is heavy the shoulder motion is not negligible. The current locking mechanism has a fixed locked angle, meaning the only way to change it is by replacing the rigid parts on the cuffs; this mechanism can be improved by allowing for a variable angle lock to account to the user's lifting styles.

Regarding the ergonomics of the exosuit, shoulder pads and a waist strap were installed to distribute the forces on the user, however an analysis of the force distribution along the interface between the device and the user would provide more information for future ergonomic human-robot interfaces.

The VRM can be improved in several ways. The currently limited set of commands could be extended to include also user-defined commands that would allow a more personalised experience (e.g. using natural language processing APIs, such as Google's Speech-to-Text API). However, this would require additional on-board computational power.

A possible limitation to using voice recognition is the high level of noise in some industrial environments. In this study, the use of a limited set of single-word vocal commands contributes to more robust voice recognition. However, if the complexity of the commands should be increased to provide a more intuitive interface, some technological adaptations may be needed to increase the robustness of the VRM against noise. For example, based on the noise characteristics in the specific industrial environment, active noise cancellation techniques or noise-resilient recognition algorithms [30] may be adopted.

5. Conclusions

We have developed a lightweight, industrial, wearable device with a VRM and found that it reduced the muscular activity of the BB and AD muscles when performing industrial tasks with a light load (7kg). There are three major contributions presented in this paper: the first contribution is an underactuated mechanism, utilizing a mechanical lock, which allowed the optimization of the mass of the exosuit; the second contribution is a passive DoF that allowed free motion of the arm in the transverse plane and improved the ergonomics of the device; the third contribution is the VRM, which is a hands-free HMI, that was implemented to control the device.

Future work for this device will focus thoroughly on characterizing the ergonomics of the device, in addition to measuring the affect of the compliance of the suit on the kinematics.

Declaration of interests

The authors declare that they have no known competing financial interests or personal relationships that could have appeared to influence the work reported in this paper.

CRediT authorship contribution statement

Yongtae G. Kim: Conceptualization, Methodology, Software, Formal analysis, Investigation, Writing - original draft. **Kieran Little:** Methodology, Formal analysis, Investigation, Writing - original draft, Writing - review & editing. **Bernardo Noronha:** Methodology, Formal analysis, Investigation, Writing - original draft, Writing - review & editing. **Michele Xiloyannis:** Conceptualization, Methodology, Formal analysis, Investigation, Writing - original draft, Writing - review & editing. **Lorenzo Masia:** Conceptualization, Methodology, Investigation, Resources, Writing - review & editing, Supervision, Project administration, Funding acquisition. **Dino Accoto:** Conceptualization, Methodology, Resources, Writing - review & editing, Supervision, Project administration.

Acknowledgments

This work was partially supported by the "Smart Exosuits for Human Augmentation in Industrial Working Environment" project funded by Parts Precision Technology (S) Pte Ltd (project definition: M4062147).

Appendix A. Wire length for the shoulder flexion

Below are the equations of the length of the wire as a function joint angles (q_s, q_e):

$$l_{ws}(q_s) = \sqrt{l_{wsx}^2 + l_{wsy}^2} \tag{A.1}$$

$$l_{wsx}(q_s) = l_{pv} - (l_0 - l_a)sin(q_s) - dcos(q_s) \tag{A.2}$$

$$l_{wsy}(q_s) = -l_{ph} - (l_0 - l_a)cos(q_s) + dsin(q_s) \tag{A.3}$$

$$\Delta l_w = r_{pulley}\Delta\theta_m \tag{A.4}$$

$$l_{ws}^i = \sqrt{((l_0 - l_a) + l_{ph})^2 + (l_{pv} - d)^2} \tag{A.5}$$

where l_{ws} is the wire length for the shoulder flexion, Δl_w is the change of the wire length by motor rotation, r_{pulley} is the radius of the pulley, and l_{ws}^i is the shoulder wire length of the lock point ($q_s = 0°$, $q_e = 90°$). The required motor counts ($\Delta\theta_m$) for reaching target wire difference (Δl_w) can be calculated by the difference of the wire lengths ($l_{ws}(q_s) - l_{ws}^i$).

$$l_{we}(q_e) = \sqrt{l_a^2 + l_b^2 - 2l_a l_b cos(q_e)} \tag{A.6}$$

$$q_e(l_{we}) = cos^{-1}\left(\frac{l_a^2 + l_b^2 - l_{we}^2}{2l_a l_b}\right) \tag{A.7}$$

where l_{we} is the wire length for the elbow flexion. The wire length for the elbow (l_{we}) can be obtained by computing the difference between amount of winding and required shoulder wire length ($l_{we} = l_w(C2 \rightarrow C1) - l_{ws}$). Then the elbow angle of C1 can be obtained by the equation above.

Supplementary material

Supplementary material associated with this article can be found, in the online version, at 10.1016/j.rcim.2020.101995

References

[1] M.P. de Looze, T. Bosch, F. Krause, K.S. Stadler, L.W. O'Sullivan, Exoskeletons for industrial application and their potential effects on physical work load, Ergonomics 5 (2016) 671–681, https://doi.org/10.1080/00140139.2015.1081988.

[2] R. Bogue, Exoskeletons a review of industrial applications, Industrial Robot 45 (5) (2018) 585–590, https://doi.org/10.1108/IR-05-2018-0109.

[3] G. Michalos, N. Kousi, P. Karagiannis, C. Gkournelos, K. Dimoulas, S. Koukas, K. Mparis, A. Papavasileiou, S. Makris, Seamless human robot collaborative assembly an automotive case study, Mechatronics 55 (2018) 194–211, https://doi.org/10.1016/j.mechatronics.2018.08.006.

[4] A. Campeau-Lecours, P.-L. Belzile, T. Lalibert, S. Foucault, B. Mayer-St-Onge, D. Gao, C. Gosselin, An articulated assistive robot for intuitive hands-on-payload manipulation, Robotics and Computer-Integrated Manufacturing 48 (2017) 182–187, https://doi.org/10.1016/j.rcim.2017.04.003.

[5] G. Castelli, E. Ottaviano, P. Rea, A cartesian cable-suspended robot for improving end-users mobility in an urban environment, Robotics and Computer-Integrated Manufacturing 30 (3) (2014) 335–343, https://doi.org/10.1016/j.rcim.2013.11.001.

[6] S.A. Matthaiakis, K. Dimoulas, A. Athanasatos, K. Mparis, G. Dimitrakopoulos, C. Gkournelos, A. Papavasileiou, N. Fousekis, S. Papanastasiou, G. Michalos, G. Angione, S. Makris, Flexible programming tool enabling synergy between human and robot, Procedia Manufacturing 11 (2017) 431–440, https://doi.org/10.1016/j.promfg.2017.07.131. 27th International Conference on Flexible Automation and Intelligent Manufacturing, FAIM2017, 27-30 June 2017, Modena, Italy

[7] K. Huysamen, M. de Looze, T. Bosch, J. Ortiz, S. Toxiri, L.W. O'Sullivan, Assessment of an active industrial exoskeleton to aid dynamic lifting and lowering manual handling tasks, Applied Ergonomics (2017) 125–131, https://doi.org/10.1016/j.apergo.2017.11.004.

[8] B. Kim, A.D. Deshpande, An upper-body rehabilitation exoskeleton harmony with an anatomical shoulder mechanism: Design, modeling, control, and performance evaluation, The International Journal of Robotics Research 36 (4) (2017) 414–435, https://doi.org/10.1177/0278364917706743.

[9] M. Abdoli-E, M.J. Agnew, J.M. Stevenson, An on-body personal lift augmentation device (PLAD) reduces EMG amplitude of erector spinae during lifting tasks, Clinical Biomechanics 21 (5) (2006) 456–465, https://doi.org/10.1016/j.clinbiomech.2005.12.021.

[10] K. Huysamen, T. Bosch, M. de Looze, K.S. Stadler, E. Graf, L.W. O'Sullivan, Evaluation of a passive exoskeleton for static upper limb activities, Applied Ergonomics (2017) 148–155, https://doi.org/10.1016/j.apergo.2018.02.009.

[11] J. Theurel, K. Desbrosses, T. Roux, A. Savescu, Physiological consequences of using an upper limb exoskeleton during manual handling tasks, Applied Ergonomics (2017) 211–217, https://doi.org/10.1016/j.apergo.2017.10.008.

[12] H. Kobayashi, T. Aida, T. Hashimoto, Muscle suit development and factory application, International Journal of Automation Technology 3 (6) (2016) 709–715, https://doi.org/10.20965/ijat.2009.p0709.

[13] B. Otten, R. Weidner, A. argubi-wollesen, evaluation of a novel active exoskeleton for tasks at or above head level, IEEE Robotics and Automation Letters 3 (3) (2018) 1, https://doi.org/10.1109/lra.2018.2812905.

[14] M. Xiloyannnis, D. Chiaradia, A. Frisoli, L. Masia, Physiological and kinematic effects of a soft exosuit on arm movements, Journal of NeuroEngineering and Rehabilitation 16(29). 10.1186/s12984-019-0495-y.

[15] K. Little, C.W. Antuvan, M. Xiloyannis, A.P.S. d. N. Bernardo, Y.G. Kim, L. Masia, D. Accoto, IMU-based assistance modulation in upper limb soft wearable exosuits, 2019 IEEE 16th International Conference on Rehabilitation Robotics (ICORR), IEEE, 2019, pp. 1197–1202.

[16] Y. Zhang, V. Arakelian, Design of a passive robotic exosuit for carrying heavy loads, IEEE-RAS International Conference on Humanoid Robots (2018) 860–865, https://doi.org/10.1109/HUMANOIDS.2018.8624956.

[17] S. Papanastasiou, N. Kousi, P. Karagiannis, C. Gkournelos, A. Papavasileiou, K. Dimoulas, K. Baris, S. Koukas, G. Michalos, S. Makris, Towards seamless human robot collaboration: integrating multimodal interaction, International Journal of Advanced Manufacturing Technology 105 (9) (2019) 3881–3897, https://doi.org/10.1007/s00170-019-03790-3.

[18] K. Kiguchi, Y. Hayashi, An EMG-based control for an upper-limb, IEEE Transactions on Systems, Man, and Cybernetics, Part B (Cybernetics) 42 (4) (2012) 1064–1071, https://doi.org/10.1109/TSMCB.2012.2185843.

[19] J.N. Pires, Robot-by-voice: Experiments on commanding an industrial robot using the human voice, Industrial Robot 32 (6) (2005) 505–511, https://doi.org/10.1108/01439910510629244.

[20] Y.G. Kim, M. Xiloyannis, D. Accoto, L. Masia, Development of a soft exosuit for industrial applications, 2018 7th IEEE International Conference on Biomedical Robotics and Biomechatronics (Biorob), (2018), pp. 324–329.

[21] S. Rodgers, Metabolic indices in materials handling tasks, Safety in Manual Materials Handling: Report on International Symposium, Safety in Manual Materials Handling, State University of New York at Buffalo, 1978, pp. 52–56.

[22] T.K. Chuan, M. Hartono, N. Kumar, Anthropometry of the singaporean and indonesian populations, International Journal of Industrial Ergonomics 40 (6) (2010) 757–766, https://doi.org/10.1016/j.ergon.2010.05.001.

[23] J. Jin, N. Gans, Parameter identification for industrial robots with a fast and robust trajectory design approach, Robotics and Computer-Integrated Manufacturing 31 (2015) 21–29, https://doi.org/10.1016/j.rcim.2014.06.004.

[24] D. Stegeman, H. Hermens, Standards for surface electromyography: The european project surface emg for non-invasive assessment of muscles (seniam), Enschede: Roessingh Research and Development, (2007), pp. 108–112.

[25] D.E. Barkana, J. Das, F. Wang, T.E. Groomes, N. Sarkar, Incorporating verbal feedback into a robot-assisted rehabilitation system, Robotica 29 (3) (2011) 433–443, https://doi.org/10.1017/S0263574710000275.

[26] A. Poncela, L. Gallardo-Estrella, Command-based voice teleoperation of a mobile robot via a human-robot interface, Robotica 33 (1) (2015) 1–18, https://doi.org/10.1017/S0263574714000010.

[27] J.H. Kim, K. Abdel-Malek, J. Yang, R.T. Marler, Prediction and analysis of human motion dynamics performing various tasks, International Journal of Human Factors Modelling and Simulation 1 (1) (2006) 69–94, https://doi.org/10.1504/IJHFMS.2006.011683.

[28] D. Landin, M. Thompson, M.R. Jackson, Actions of the biceps brachii at the shoulder: A review, Journal of Clinical Medicine Research 9 (8) (2017) 667–670, https://doi.org/10.14740/jocmr2901w.

[29] K. Schmidt, J.E. Duarte, M. Grimmer, A. Sancho-Puchades, H. Wei, C.S. Easthope, R. Riener, The myosuit: Bi-articular anti-gravity exosuit that reduces hip extensor activity in sitting transfers, Frontiers in neurorobotics 11 (2017) 57, https://doi.org/10.3389/fnbot.2017.00057.

[30] J. Li, L. Deng, Y. Gong, R. Haeb-Umbach, An overview of noise-robust automatic speech recognition, IEEE/ACM transactions on audio, Speech, and Language Processing 22 (2014) 745–777, https://doi.org/10.1016/j.promfg.2017.07.131.